Research Article

Journal of Environmental Nanotechnology

Performance of Ternary Blended Concrete Incorporating Micro-silica and Nano Zeolite

R. Karthikeyan[1*], P. Partheeban[1], M. Sivakumar[1], K. Suguna[2] and K. K. Gaayathiri[3]

[1]Department of Civil Engineering, Chennai Institute of Technology, TN, India
[2]Department of Civil and Structural Engineering, Annamalai University, Chidambaram, TN, India
[3]Department of Civil Engineering, Vel Tech Rangarajan Dr. Sagunthala R and D Institute of Science and Technology, Chennai, TN, India
Received: 27.06.2025 Accepted: 05.09.2025 Published: 30.09.2025
*rkarthikeyan@citchennai.net

ABSRTACT

This study investigates the performance of ternary blended concrete incorporating micro-silica and nano-zeolite as supplementary cementitious materials. The inclusion of micro-silica, known for its high pozzolanic reactivity and ultrafine particle size, helped refine the pore structure and enhanced the bond between cement paste and aggregates. Nano-zeolite, due to its high surface area and nanostructure, further improved hydration kinetics and contributed to better densification of the matrix. Micro-silica was used at a constant dosage of 10%, while nano-zeolite replaced cement at varying levels of 5%, 10%, and 15% by weight. A total of 36 specimens were cast, including cubes (150 × 150 × 150 mm), cylinders (150 × 300 mm), and prisms (150 × 250 × 500 mm). Fifteen specimens served as control samples made with conventional concrete, while the remaining 21 were prepared using micro-silica and nano-zeolite. Mechanical and durability tests were conducted on all concrete mixes. The results demonstrated significant improvements in compressive strength, flexural strength, and modulus of elasticity. In terms of durability, notable reductions were observed in sorptivity and chloride ion permeability.

Keywords: Blended concrete; Sorptivity; Micro-silica; Nano-Zeolite; Durability; Strength.

1. INTRODUCTION

Concrete is the most widely used construction material due to its adaptability, strength, and cost-effectiveness. However, its long-term performance is challenged by durability-related issues such as permeability, chemical attacks, and water absorption. Over the years, researchers have explored various supplementary cementitious materials (SCMs) to enhance concrete's performance, among which micro-silica and nano-silica have shown considerable promise. Micro-silica (also known as silica fume), an ultrafine byproduct of the silicon and ferrosilicon alloy industry, has been effectively used to refine pore structure, enhance compressive strength, and decrease permeability. Its incorporation improves concrete's mechanical and durability characteristics by densifying the interfacial transition zone and promoting the formation of additional calcium silicate hydrate (C–S–H) (Ashish, 2020; Mansoori *et al.* 2021). Numerous studies have confirmed the role of micro-silica in improving concrete properties. For instance, Kannan *et al*. (2019) showed that micro-silica substantially enhances chloride resistance. Similarly, Li *et al.* (2017) demonstrated that the simultaneous use of micro- and nano-silica decreased carbonation depth, while Singh and Sarvade (2018) noted improvements in acid and sulfate resistance. Moreover, Collepardi *et al.* (2004) optimized silica fume and fly ash combinations for high-performance concrete, highlighting micro-silica's synergetic role in ternary blends. Advancements in nanotechnology have introduced nano-silica as a next-generation additive in concrete. Its high surface area and reactivity accelerate hydration and improve early-age strength development. Reviews by Papic *at el.* (2021), Patil *at el.* (2023), Liu *et al*. (2021), and Sanchez and Sobolev, (2010) consolidated the wide-ranging effects of nano-silica, including pore refinement, strength enhancement, and durability improvement. Experimental studies (Bi *et al*. 2012; Ji *et al.* 2005) have further validated that nano-silica significantly reduces permeability and increases compressive strength at lower dosages. Rajput and Pimplikar, (2022) and Athira and Shanmugapriya (2022) found that nano-silica reduces water absorption in high-grade concrete mixes. Huang *et al.* (2022) and Huang *et al*. (2020) confirmed improved resistance to sulfate attack in nano-silica-modified concrete. Additionally, studies by Kong *et al*. (2012) and Sobolev and Gutierrez (2005) indicated that nano-silica contributes to concrete densification and microstructural integrity, particularly when combined with other SCMs. In parallel, zeolite, a natural pozzolan with a crystalline aluminosilicate structure, has emerged as a sustainable SCM. It exhibits high pozzolanic activity and ion-exchange properties beneficial for improving concrete's resistance to chemical attacks and chloride ion penetration. Mohsen *et al.* (2019) demonstrated that replacing cement with zeolite, in combination with metakaolin, improved both strength and durability. Though traditionally used in micron-scale form, interest in nano-zeolite is growing due to its

enhanced reactivity and surface properties (Zarehparvar and Eskandari, 2024). Recent research has focused on combining nano-silica and other SCMs to create ternary blended concrete, aiming to capitalize on the synergistic effects of both micro- and nano-scale materials. Bharat *et al.* (2024) reported that blends of nano-silica and fly ash improved mechanical and durability behavior through microstructure densification. Similarly, Biolzi and Cattaneo, (2011) and Wong *et al.* (2018) highlighted the enhanced durability and rheological performance in lightweight and self-compacting concretes containing micro- and nano-silica. The use of nano-zeolite in conjunction with micro-silica may offer significant benefits by promoting early-age strength, reducing permeability, and improving long-term durability, as discussed in the reviews by Ashish, (2020) and Papic and Patil (2023). Among the efforts to test supplementary cementitious materials, the investigation by Senthilkumar *et al.* (2023) on the use of eggshell powder and incinerated eggshell powder as partial cement replacements is notable.

The present study investigates the performance of ternary blended concrete incorporating micro-silica and nano-zeolite, focusing on both mechanical properties (compressive strength, flexural strength, and modulus of elasticity) and durability parameters (water absorption, acid resistance, porosity, and rapid chloride penetration).

2. EXPERIMENTAL STUDIES

2.1 Materials

The materials used in this work include Ordinary Portland Cement (OPC), micro-silica, nano-zeolite, potable water, coarse aggregate with a maximum size of 20 mm, fine aggregate, and a super-plasticizer.

2.1.1 Cement

Ordinary Portland Cement of 53 grade was used in the preparation of concrete. The properties of the cement conform to IS 12269:2013 specifications. The specific gravity of the cement was found to be 3.15, and the compressive strength was recorded at 35 MPa, which falls within the permissible range of 30–50 MPa. The tensile strength was 3.5 MPa, aligning with the typical range of 10–15% of the compressive strength (fck). The fineness, measured using the air permeability method, was 6.50%, which satisfies the requirement of being less than 10%. The normal consistency was determined to be 32%, falling within the standard range of 30–35%. The initial and final setting times were 50 minutes and 420 minutes, respectively, meeting the required limits of more than 30 minutes for the initial and less than 600 minutes for the final setting time. The chemical composition included 18.3% silicon dioxide (SiO_2) and 3.3% gypsum, both of which are within acceptable limits as per the standards.

2.1.2 Zeolite

The zeolite used in this experimental investigation was procured from ASTRRA Chemicals, Chennai. The specific gravity of the zeolite was found to be 2.2, and its fineness modulus was 3.3%. The material exhibited a water absorption capacity of 1.5%, and it appeared as a greenish-grey powder. The bulk density of the zeolite ranged between 800 and 1041 kg/m³. Additionally, the degree of pozzolanic reactivity was recorded at 15%, confirming its suitability as a supplementary cementitious material in concrete

2.1.3 Silica Fume

Silica fume, also known as micro-silica, is a by-product generated during the production of silicon metal or ferrosilicon alloys. In this experimental study, the silica fume was supplied by ASTRRA Chemicals, Chennai. The material appeared as a white, powdery substance and had a specific gravity of 1.5. Its fineness modulus was measured at 2.68, and the water absorption was found to be 1.7%. The degree of pozzolanic reaction at 28 days was recorded at 10%, indicating its effectiveness as a reactive pozzolanic material in concrete.

2.1.4 Fine Aggregate

Fine aggregate used in the concrete specimens had a specific gravity of 2.68 and was selected in accordance with IS 383:1970. Based on the grading, it fell under Zone II classification. The fineness modulus of the fine aggregate was 2.7, and the water absorption capacity was recorded at 1.02%, as shown in Fig. 1.

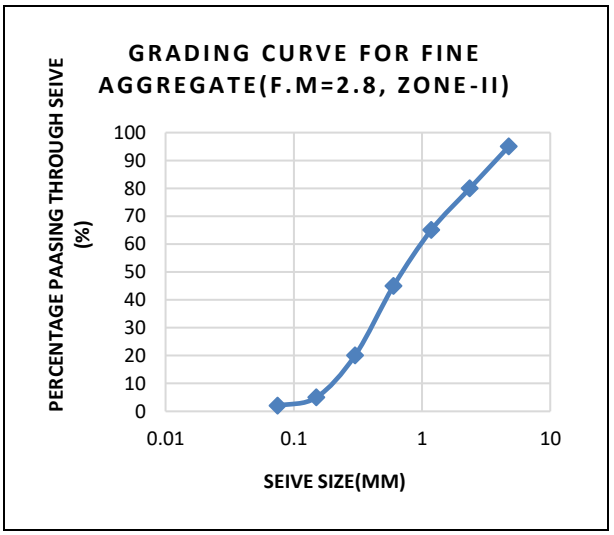


Fig. 1: Grading curve for fine aggregate

2.1.5 Coarse Aggregate

The coarse aggregate used in this study had a maximum size of 20 mm and was tested by IS: 383-1970.

The specific gravity of the coarse aggregate was found to be 2.78, with a fineness modulus of 7.22, as shown in Fig. 2. The water absorption capacity was recorded at 0.83%.

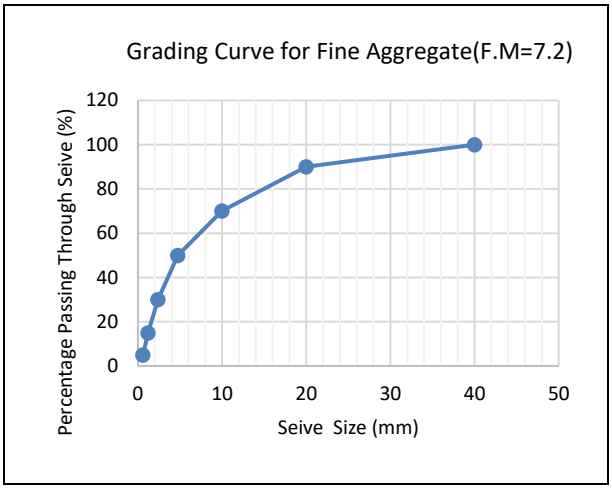


Fig. 2: Grading curve for coarse aggregate

2.1.6 Super Plasticizer

A superplasticizer based on sulphonated naphthalene (Fig. 3) was used in this study, which complies with ASTM C494 standards. The superplasticizer was supplied by Fosroc Chemicals, Chennai. Preliminary trials were conducted to determine the optimal dosage for various mix combinations, taking into account both workability and strength requirements. The superplasticizer appeared as a brown liquid, had a specific gravity of 1.18 at 25°C, and contained no chlorides.

2.1.7 Water

Potable water conforming to IS 456:2000 was used for preparing the concrete specimens. A water-to-binder ratio of 0.48 was used in each mix.

2.1.8 Material Characterization Based on Chemical Composition

The chemical compositions of zeolite, micro-silica, and OPC used in this study are presented in Table 1. As shown, micro-silica contains a significantly higher percentage of silica (SiO_2), ranging from 85–98%, compared to 55–70% in zeolite and 19–25% in OPC cement. Zeolite is notably rich in alumina (Al_2O_3) and contains moderate amounts of alkali oxides (Na_2O and K_2O), contributing to its pozzolanic activity. In contrast, OPC has the highest calcium oxide (CaO) content (60–67%), which is essential for hydration reactions. The loss on ignition (LOI) values also vary, indicating differences in unburnt material and moisture content across the materials.

Table 1. Chemical composition of cement, micro-silica and nano-zeolite

Content	SiO_2	Al_2O_3	Fe_2O_3	CaO	MgO	Na_2O	K_2O	SO_3	Loss on Ignition
Zeolite	55–70	12–20	0.5–2	2–8	0.5–2	0.5–6	0.5–4	—	8–14
Micro-Silica	85–98	0.2–0.8	0.1–0.3	0.1–0.5	0.1–0.3	0.2–0.8	0.2–1.0	—	1–3
OPC Cement	19–25	4–8	2–5	60–67	0.5–4	0.2–0.8	0.2–1.3	1–3	1–4



Fig. 3: Superplasticizer



Fig. 4: Ingredients used in the concrete mix for preparing test specimens

2.2 Raw Materials

Raw materials used in the preparation of concrete mix are shown in Fig. 4. These materials include coarse aggregate, fine aggregate, cement, zeolite, silica fume, and water.

The classification of all the test samples is presented in Table 2.

2.4 Mix Design

The concrete mix was designed with a control mix ratio of 1:1.8:2.9 for cement, fine aggregate, and coarse aggregate, respectively. The mix utilized 380 kg/m^3 of cement, 715 kg/m^3 of fine aggregate, 1130 kg/m^3 of coarse aggregate, and 186 litres of water per cubic meter, resulting in a water–cement ratio of 0.49. Table 3 presents the detailed mix design proportions for all the tested specimens. The control concrete (CC) consisted of 380 kg/m^3 of cement, 186 kg/m^3 of water, 715 kg/m^3 of fine aggregate, and 1101 kg/m^3 of coarse aggregate, with no supplementary materials. In the modified mixes, partial replacements of cement were made using micro-silica and nano-zeolite. For ZS_1, 15% of the cement was replaced by 10% micro-silica (38 kg/m^3) and 5% nano-zeolite (19 kg/m^3), resulting in a reduced cement content of 323 kg/m^3. In ZS_2, 20% of the cement was substituted equally by 10% micro-silica and 10% nano-zeolite, with the original cement content of 380 kg/m^3 maintained. ZS_3 included a 25% replacement of cement with 10% micro-silica and 15% nano-zeolite (57 kg/m^3), also retaining the original cement quantity. The water–cement ratio remained consistent at 0.49 for all mixes.

Table 2. Classification of test specimen

Specimens	Description
CC	Control concrete specimen with 0% of silica fume and 0% Zeolite
ZS_1	Specimen with 5% Silica fume and 10% Zeolite
ZS_2	Specimen with 10% Silica fume and 10% Zeolite
ZS_3	Specimen with 15% Silica fume and 10% Zeolite

Table 3. Mix design proportion for all specimens

Specimen	Cement (kg/m³)	Water (kg/m³)	Fine Aggregate (kg/m³)	Coarse Aggregate (kg/m³)	Micro-Silica	Nano-Zeolite	Water-Cement Ratio
CC	380	186	715	1130	0	0	0.49
ZS_1	323	186	715	1130	19	38	0.49
ZS_2	304	186	715	1130	38	38	0.49
ZS_3	285	186	715	1130	57	38	0.49

2.5 Stages of Concrete Specimens Casting

The step-by-step procedure of casting concrete specimens is shown in Fig. 5. It begins with the weighing and mixing of ingredients, followed by placing the fresh concrete into cube and cylinder moulds. The concrete is then compacted to remove air voids, and the surfaces are levelled. A slump test is conducted to assess the workability of the mix. After setting, the specimens are carefully demoulded and cured. Once curing is complete, the specimens are ready for strength testing.

2.4 Test Methods

2.4.1 Compressive Strength

The compressive strength test was conducted after 28 days of water curing to evaluate the load-bearing capacity of the concrete specimens. For this purpose, standard cube specimens of size 150 mm × 150 mm × 150 mm were cast for each of the three concrete mix variations. The testing procedure adhered to the guidelines provided in IS 516:2004, which outlines the method of tests for the strength of concrete. Before testing, the specimens were removed from the curing tank, surface dried, and placed in a compression testing machine. The load was applied uniformly and gradually until failure occurred, and the maximum load was recorded. This value was then used to calculate the compressive strength. The test setup used for performing the cube compression test is illustrated in Fig. 6.



Fig. 5: Various stages of casting specimens



Fig. 6: Test setup for measuring the compressive strength of a concrete cube specimen



Fig. 7: Test setup for measuring the flexural strength of a concrete prism specimen

2.4.2 Flexural Strength

Flexural strength test was carried out on prism specimens after 28 days of water curing in accordance with IS 516:2004. A total of eleven prisms, each measuring 100 mm × 100 mm × 500 mm, were cast; three for each concrete mix variation. Before testing, the prisms were surface-dried to remove excess moisture. Tests were performed using a flexural testing machine in a three-point bending configuration, with a support span of 500 mm. The load was applied at a constant rate of 0.05 MPa/s until fracture occurred. The test setup for the prism bending test is shown in Fig. 7. The maximum load at failure (P) was recorded for each specimen, and the modulus of rupture (flexural strength), f_{cr}, was calculated using

$$f_{cr} = 2PL/bd \quad \ldots (1),$$

where

P maximum applied load (N)
L span length (500 mm)
b prism width (100 mm)
d = prism depth (100 mm)

2.4.3 Modulus of Elasticity Test on Cylinders

The modulus of elasticity of concrete was calculated using cylindrical specimens tested under axial compression in a 1000 kN capacity universal testing machine. For each mix type, three identical cylinders were tested, and the average value of these three readings was considered the representative result for that particular group. Before the test, both the upper and lower faces of each cylinder were carefully ground and levelled to ensure smooth and parallel surfaces, thereby minimising the risk of eccentric loading and ensuring uniform stress distribution during the test. The cylinders were positioned vertically in the testing machine, and axial load was applied at a controlled rate as per the relevant standard. Fig. 8 shows the detailed test configuration used in this investigation, including the alignment and placement of specimens. The modulus of elasticity was calculated from the stress-strain relationship obtained during loading within the elastic range of the material.



Fig. 8: Test setup for measuring the modulus of elasticity of a concrete cylinder specimen

2.4.4 Sorptivity

The sorptivity test was determined on 100 mm diameter and 50 mm thick concrete discs after 28 days of curing. The sides and top surfaces were sealed to ensure unidirectional water flow, as shown in Fig. 9. The specimens were oven-dried at 50 ± 2°C until a constant weight was achieved, and then cooled to room

temperature. The bottom surface was exposed to 2–3 mm of water, and the mass gain was recorded at regular intervals. Sorptivity was calculated from the slope of the plot between cumulative water absorption and the square root of time, indicating the rate of capillary suction in concrete.



Fig. 9: Sorptivity test arrangement for a concrete disc specimen

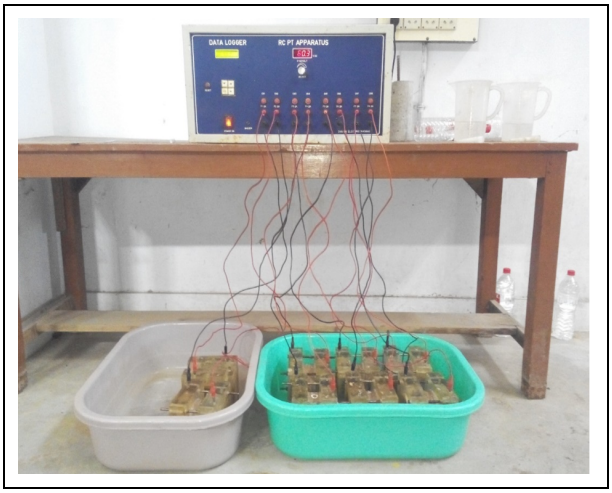


Fig. 10: Rapid chloride penetration test apparatus for concrete specimens

2.4.5 Rapid Chloride Penetrating Test

In the ASTM C 1202 test, a water-saturated, 51-mm thick and 102-mm wide concrete specimen was subjected to a 60 V applied DC voltage for 6 hours using the apparatus shown in Fig. 10. In one reservoir, 3.0% (30 g/L) of NaCl and in the other reservoir 0.3 N (12 g/lit) of NaOH solutions were filled. The total charge passed was determined, and this was used to rate the concrete according to the criteria included in Table 4. This test, originally developed by Whiting [1981], is commonly (and inaccurately) referred to as the "Rapid Chloride Permeability" test. The total charge passed is a measure of the electrical conductivity of the concrete during the test period.

$$Q = 900 (I_0 + 2I_{30} + 2I_{60} + 2I_{90} + \ldots\ldots\ldots + 2I_{300} + 2I_{330} + I_{360}) \quad \ldots (2),$$

where,

Q – Charge passed (Coulombs)

I_0– Current (amperes) immediately after voltage is applied

I_t– Current (amperes) at t min after voltage is applied

Table 4. Chloride ion penetrability based on the charge passed

Charge Passed (Coulombs)	Chloride Ion Penetrability
> 4000	High
2000 – 4000	Moderate
1000 – 2000	Low
100 – 1000	Very Low

3. RESULTS AND DISCUSSION

3.1 Effect of Micro-silica and Nano-zeolite on Compressive Strength

The Compressive strength was observed in the ternary blended concrete is presented in Table 5. The ZS_2 specimens, in which 10 % of the cement was replaced by zeolite and 10 % by micro-silica, exhibited a 17.38 % increase in compressive strength over the control mix as shown in Fig. 11. This strength gain is attributed to the dual pozzolanic reactions of micro-silica and zeolite, which consume calcium hydroxide to form additional calcium silicate hydrate (C–S–H) and calcium alumino-silicate hydrate (C–A–S–H) gels, thereby refining the pore structure. At the same time, the ultrafine micro-silica particles and porous zeolite act as fillers, packing into capillary voids and reducing overall porosity. Their surfaces provide abundant nucleation sites for hydration products, enhancing the density and bond strength of the interfacial transition zone around aggregates. Together, these effects produce a denser, more homogeneous microstructure that resists crack initiation and propagation under load.

3.2 Effect of Micro-silica and Nano-zeolite on Flexural Strength

The flexural strength of the ternary-blended concrete is presented in Table 6, and the corresponding percentage increase is shown in Fig. 12. The ZS_2 specimens (where 10 % of the cement was replaced by zeolite and 10 % by micro-silica) exhibited the highest flexural capacity, with an increase of 8.35% over the control mix. This enhancement is likewise attributed to the dual pozzolanic activity of micro-silica and zeolite, which consume calcium hydroxide to produce additional C–S–H and C–A–S–H gels, thereby refining the pore structure and stiffening the cement matrix. Simultaneously, the ultrafine micro-silica particles and

porous zeolite act as micro-fillers, occluding capillary voids and reducing overall porosity. Their high-surface-area interfaces further serve as nucleation sites for hydration products, strengthening the interfacial transition zone around aggregates. Under bending loads, this denser, more homogeneous microstructure improves stress transfer across microcracks and delays crack initiation and propagation, resulting in significantly higher flexural performance.

Table 5. Compressive strength of tested cube concrete specimens

S. No.	Designation of Specimen	Zeolite (%)	Silica Fume (%)	Compressive Strength (N/mm^2)
1.	CC	0	10	26.35
2.	ZS_1	5	10	27.11
3.	ZS_2	10	10	30.93
4.	ZS_3	15	10	29.48

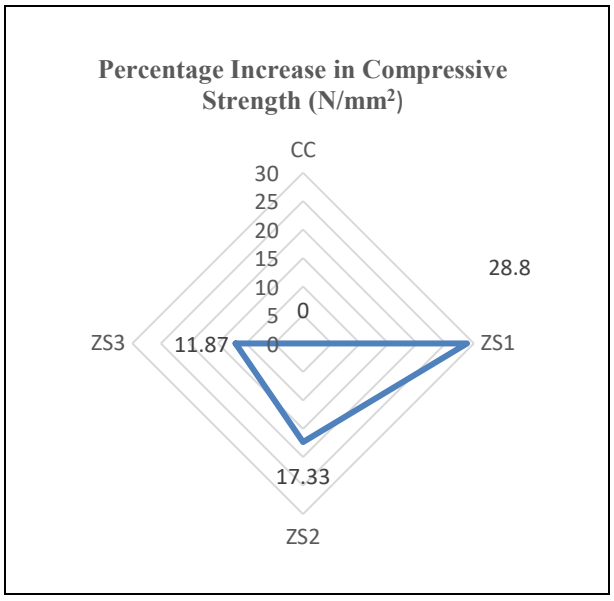


Fig. 11: Enhancement in compressive strength (%) observed for ternary blended concrete compared with the control mix

Table 6. Flexural strength of tested concrete prism specimens

S. No.	Designation of Specimen	Zeolite (%)	Silica Fume (%)	Flexural Strength (N/mm^2)
1.	CC	0	0	3.59
2.	ZS_1	10	5	3.64
3.	ZS_2	10	10	3.89
4.	ZS_3	10	15	3.80

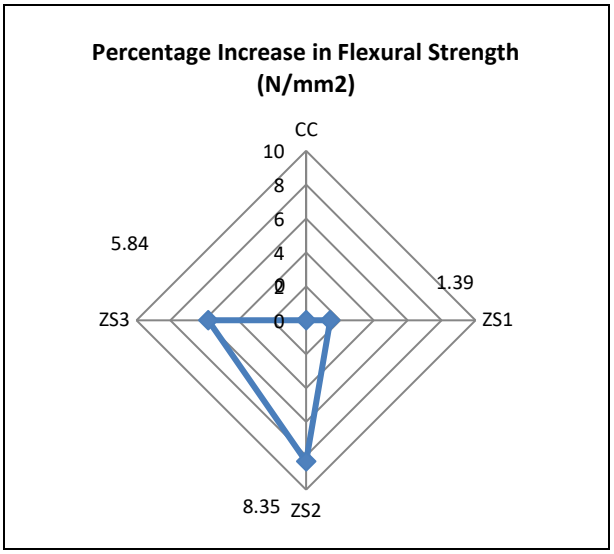


Fig. 12: Enhancement in flexural strength (%) observed for ternary blended concrete compared with the control mix

3.3 Effect of Micro-silica and Nano-zeolite on Modulus of Elasticity

The modulus of elasticity of the ternary-blended concrete is presented in Table 7, and the corresponding percentage increase is shown in Fig. 13. The ZS_2 specimens exhibited the highest modulus of elasticity, with an increase of 8.35% over the control mix. The notably higher modulus in ZS_2 arises from the optimal balance between pozzolanic activity and matrix densification at the 10 % replacement level. At this proportion, the additional calcium silicate hydrate (C–S–H) and calcium alumino-silicate hydrate (C–A–S–H) gels generated by zeolite and micro-silica most effectively fill capillary pores and stiffen the cement paste. Below this level (ZS_1), fewer pozzolanic products are formed; above it (ZS_3), excessive zeolite begins to dilute the cement matrix. Consequently, ZS_2 delivers the peak combination of increased binder stiffness and reduced porosity, resulting in the highest elastic modulus among the tested mixes.

Table 7. Modulus elasticity of tested concrete cylinder specimens

S. No.	Designation of Specimen	Zeolite (%)	Silica Fume (%)	Elasticity Modulus (GPa)
1.	CC	0	0	25.67
2.	SZ_1	5	10	26.03
3.	SZ_2	10	10	27.81
4.	ZS_3	15	10	27.15

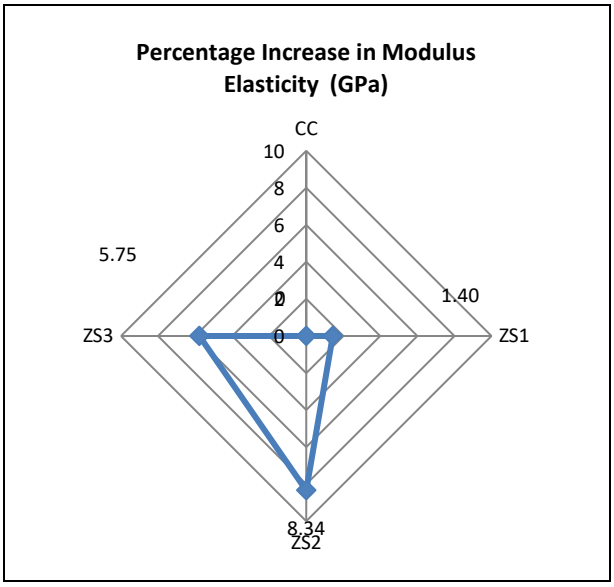


Fig. 13: Enhancement in modulus of elasticity (%) observed for ternary blended concrete compared with the control mix

Table 8. Sorptivity test of tested concrete cylinder specimen

S. No.	Designation of Specimen	Zeolite (%)	Silica Fume (%)	Sorptivity Values mm/min
1.	CC	0	0	1.95
2.	ZS_1	10	5	1.92
3.	ZS_2	10	10	1.80
4.	ZS_3	10	15	1.85

3.4 Effect of Micro-silica and Nano-zeolite on Sorption

The sorptivity test results for all mixes are presented in Table 8, and the percentage reduction in sorptivity is illustrated in Fig. 14. The control concrete (CC) exhibited the highest sorptivity value of 1.95 mm/min, indicating greater capillary absorption and a more porous microstructure. The ZS_1 (5 % zeolite, 10 % micro-silica) showed a slightly reduced sorptivity of 1.92 mm/min, representing a 1.55% decrease compared to the control. The ZS_2 mix (10 % zeolite, 10 % micro-silica) demonstrated the lowest sorptivity, measured at 1.80 mm/min, corresponding to a 7.7 % reduction. Meanwhile, the ZS_3 composition (15 % zeolite, 10 % micro-silica) recorded, achieving a 5.1 % decrease. The significantly lower sorptivity in the ZS_2 mix can be attributed to the optimal replacement level of zeolite and micro-silica, which together lead to effective pore refinement and densification of the cement matrix. At the 10 % replacement level, the pozzolanic reactions produce an optimal amount of C–S–H and C–A–S–H gels, which fill microvoids and obstruct capillary channels. In contrast, ZS_1 produces a lower volume of reaction products, and in ZS_3, the excess zeolite content begins to disrupt the binder cohesion, slightly reducing the effectiveness of pore blocking. Thus, ZS_2 achieves the best performance in reducing water absorption, demonstrating the lowest sorptivity and indicating a denser, more durable concrete microstructure.

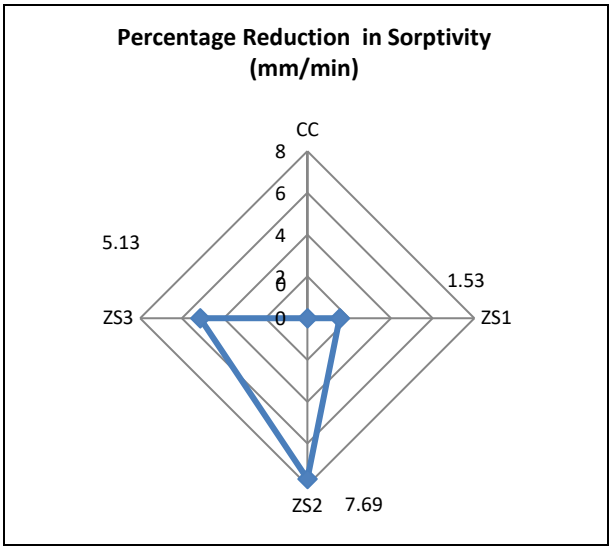


Fig. 14: Degradation in sorptivity (%) observed for ternary blended concrete compared with the control mix

3.5 Rapid Chloride Penetration Test

The RCPT results for all specimens are presented in Table 9, and the percentage reduction in charge passed is illustrated in Fig. 15. The control concrete (CC) exhibited the highest chloride permeability with a charge passed of 4000 Coulombs, indicating a relatively porous matrix and high susceptibility to chloride ion ingress. The ZS_1 mix (5% zeolite, 10% micro-silica) showed a marginal decrease to 3938 Coulombs, reflecting a 1.5% reduction. The ZS_2 mix (10% zeolite, 10% micro-silica) achieved the lowest RCPT value of 3692 Coulombs, representing a significant 7.7% reduction over the control. The ZS_3 composition (15 % zeolite, 10 % micro-silica) recorded 3795 Coulombs, indicating a 5.1 % decrease. The superior performance of ZS_2 in reducing chloride ion penetration can be attributed to its optimal balance between zeolite and micro-silica content. At this replacement level, the combined pozzolanic activity leads to the formation of additional C–S–H and C–A–S–H gels, which densify the matrix and reduce the connectivity of capillary pores. This effectively hinders ion transport through the concrete. In ZS_1, the lower zeolite content results in insufficient refinement of the pore structure, while in ZS_3, excessive zeolite begins to dilute the cementitious matrix, slightly compromising the barrier effect. As a result, ZS_2 demonstrates the best resistance to chloride penetration, confirming its potential for enhanced durability in aggressive environments.

Table 9. Rapid chloride penetration test of tested concrete cylinder specimen

S. No.	Specimen Designation	Silica Fume %	Zeolite %	RCPT (Coulombs)
1.	CC	0	0	4000
2.	ZS_1	5	10	3938
3.	ZS_2	10	10	3692
4.	ZS_3	15	10	3795

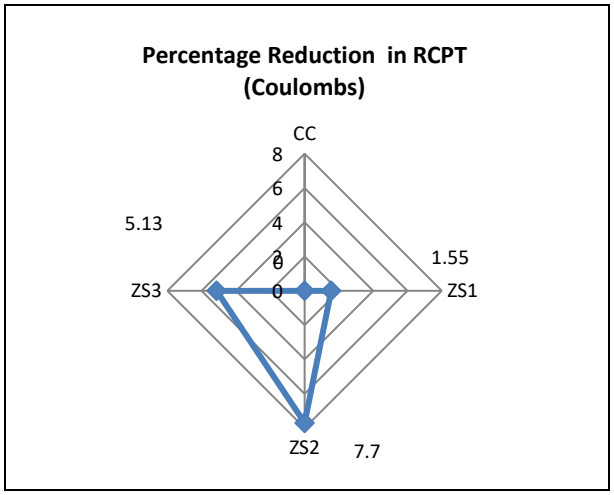


Fig. 15: Degradation in chloride penetration ion (%) observed for ternary blended concrete compared with the control mix

4. CONCLUSIONS

This study demonstrates the beneficial effects of incorporating micro-silica and zeolite as a partial substitute for cement in ternary blended concrete. At this optimized replacement level of 10% of micro silica and 10% of nano-zeolite, the mechanical performance of the concrete improved significantly. Specifically, the compressive strength increased by 12.6%, flexural strength by 8.34%, and the modulus of elasticity by 8.35% compared to the control mix. These enhancements are primarily attributed to improved bonding at the interfacial transition zone (ITZ) and the refinement of pore structures facilitated by the pozzolanic action and filler effects of micro-silica and zeolite. In addition to mechanical improvements, the ternary blended concrete also exhibited notable advancements in durability characteristics. Sorptivity was reduced by 7.69%, and chloride ion permeability (measured through the Rapid Chloride Penetration Test) decreased by 7.7%, relative to the control specimen. These reductions indicate a more refined and less permeable microstructure, which enhances the concrete's resistance to moisture ingress and aggressive ion penetration. The synergistic interaction between micro-silica and zeolite contributes to the formation of additional calcium silicate hydrate (C–S–H) and calcium alumino-silicate hydrate (C–A–S–H) gels, which densify the matrix, block capillary pores, and enhance the integrity of the cement paste. Consequently, the use of these mineral admixtures not only improves strength characteristics but also significantly bolsters the long-term durability of the concrete.

FUNDING

This research received no specific grant from any funding agency in the public, commercial, or not-for-profit sectors.

CONFLICTS OF INTEREST

The authors declare that there is no conflict of interest.

COPYRIGHT

This article is an open-access article distributed under the terms and conditions of the Creative Commons Attribution (CC BY) license (http://creativecommons.org/licenses/by/4.0/).

REFERENCES

Ashish, D. K., Influence of nano-silica and micro-silica on the properties of concrete – A review, *J. Build. Eng.*, 29, 101219(2020). https://doi.org/10.1016/j.jobe.2020.101219

Athira, P. R. and Shanmugapriya, K., Effect of red mud and nano-silica in reducing water absorption of concrete, *Mater. Today. Proc.*, 62, 2938–2943(2022). https://doi.org/10.1016/j.matpr.2022.03.342

Bharat, A., Patel, Y. and Patel, A., Performance enhancement in concrete using nano silica and fly ash: Microstructure and durability analysis, *J. Appl. Eng. Sci.*, 14(2), 212–219(2024). https://doi.org/10.2478/jaes-2024-0026

Bi, J., Pane, I., Hariandja, B. and Imran, I., The use of nano-silica for improving concrete compressive strength and durability, *Appl. Mech. Mater.*, 204–208, 4059–4062(2012). https://doi.org/10.4028/www.scientific.net/AMM.204-208.4059

Biolzi, L. and Cattaneo, S., Influence of micro- and nano-silica on mechanical properties of cement pastes, *Constr. Build. Mater.*, 25(8), 3140–3145(2011). https://doi.org/10.1016/j.conbuildmat.2011.03.031

Collepardi, M., Collepardi, S., Ongaro, D. and Troli, R., Optimisation of silica fume, fly ash, and nano-silica in high-performance concrete, *Mater. Struct.*, 37(5), 407–411(2004). https://doi.org/10.1007/BF02481605

Huang, H., Zhao, X. and Bai, Y., Effect of coarse vs. fine nano-silica on sulfate resistance of cement paste, *Constr. Build. Mater.*, 258, 120343(2020). https://doi.org/10.1016/j.conbuildmat.2020.120343

Huang, Y. W. J. and Zhou, X., Resistance to sulfate attack in concrete containing nano-silica and PVA fibers, *Constr. Build. Mater.*, 344, 128200 (2022). https://doi.org/10.1016/j.conbuildmat.2022.128200

Ji, T., Preliminary study on the water permeability and microstructure of concrete incorporating nano-SiO_2, *Cem. Concr. Res.*, 35(10), 1943–1947(2005). https://doi.org/10.1016/j.cemconres.2005.07.004

Kannan, D. M., Ganesan, K. and Obla, K. H., Chloride resistance of concrete using nano-silica and micro-silica: An experimental and statistical study, *ACI Mater. J.*, 116(4), 57–66(2019). https://doi.org/10.14359/51714514

Kong, X., Zhang, A. and Yang, W., Nano-boosted concrete: Revolutionizing strength and durability, *Mater.,* (Rio de Janeiro) 17(4), 1324–1335(2012). https://doi.org/10.1590/$S_1$517-70762012000400017

Li, G., Zhao, X. and Wang, Y., Effects of micro-silica and nano-silica on carbonation depth of concrete, *Constr. Build. Mater.*,, 154, 481–490(2017). https://doi.org/10.1016/j.conbuildmat.2017.07.209

Liu, H., Li, Q. and Yu, Y., Effect of nano-silica in concrete: A review, *Constr. Build. Mater.*, 278, 122347(2021). https://doi.org/10.1016/j.conbuildmat.2021.122347

Mansoori, A., Moein, M. M. and Mohseni, E., Effect of micro-silica on fiber-reinforced self-compacting composites containing ceramic waste, *J. Compos. Mater.*, 55(30), 4267–4277(2021). https://doi.org/10.1177/00219983211027991

Mohsen Z. P., Saghravani, S. F. and Asadollahfardi, G., Mechanical and durability properties of concrete containing zeolite mixed with metakaolin and micro-nano bubble water, *Struct. Concr.*, 20(2), 786–797. https://doi.org/10.1002/suco.201800093

Papic, M. A. and Patil, N. B., A review of the effect of nano-silica on the mechanical and durability properties of cementitious composites, *Mater. Today. Proc.*, 46, 1403–1408(2021). https://doi.org/10.1016/j.matpr.2020.08.520

Papic, M. A. and Patil, N. B., Nano-silica-modified concrete: A bibliographic analysis and comprehensive review of material properties, *Nano. Mater.*, 12(12), 1989(2023). https://doi.org/10.3390/nano12121989

Rajput, S. and Pimplikar, S. S., Nano-silica decreases water absorption in M30/M40 concrete, *Mater. Today Proc.*, 61, 260–264(2022). https://doi.org/10.1016/j.matpr.2022.05.224

Sanchez, F. and Sobolev, K., Nanotechnology in concrete – A review, *Constr. Build. Mater.*, 24(11), 2060–2071(2010). https://doi.org/10.1016/j.conbuildmat.2010.03.014

Senthilkumar, S., Sargunan, K. and Elango, S., Assessment of Strength of Concrete containing ESP and IESP as Partial Cement Replacement, *J. Environ. Nanotechnol.,* 12(3), 01-09(2023). https://doi.org/10.13074/jent.2023.09.232469

Singh, N. B. and Sarvade, A., Studies on the durability of nano-silica and silica fume blended cement mortar, *Constr. Build. Mater*, 169, 807–815(2018). https://doi.org/10.1016/j.conbuildmat.2018.03.028

Sobolev, K. and Gutierrez, M. F., How nanotechnology can change the concrete world, *Am. Ceram. Soc. Bull.*, 84(10), 14–17(2005). https://doi.org/10.1002/9780470588260.ch16

Wong, H. S., Buenfeld, N. R. and Head, M. K., Influence of micro- and nano-silica on the durability and flow properties of self-compacting lightweight concrete, *Asian. J. Civ. Eng.*, 19(8), 1013–1024(2018).

Zarehparvar, S. M. and Eskandari. N. H., Optimizing compressive strength of micro- and nano-silica concrete using statistical methods, *Civ. Eng. J.,* 10(1), 92–103(2024). https://doi.org/10.28991/cej-030939